Short-Term Spheroid Formation Enhances the Regenerative Capacity of Adipose-Derived Stem Cells by Promoting Stemness, Angiogenesis, and Chemotaxis

NAI-CHEN CHENG,[a,b,c] SZU-YU CHEN,[a] JIA-RONG LI,[b] TAI-HORNG YOUNG[b,c]

Key Words. Adult stem cells • Tissue regeneration • Cell transplantation • Angiogenesis • Cell migration

[a]Department of Surgery, National Taiwan University Hospital and College of Medicine, Taipei, Taiwan; [b]Institute of Biomedical Engineering, College of Medicine and College of Engineering and [c]Research Center for Developmental Biology and Regenerative Medicine, National Taiwan University, Taipei, Taiwan

Correspondence: Tai-Horng Young, Ph.D., Institute of Biomedical Engineering, College of Medicine, National Taiwan University, 1, Section 1, Jen-Ai Road, Taipei, Taiwan 100. Telephone: 886-2-23123456, ext. 81455; Fax: 886-2-23940049; E-Mail: thyoung@ntu.edu.tw

ABSTRACT

Adipose-derived stem cells (ASCs) represent an important source of mesenchymal stem cells for clinical application. During in vitro culture, ASCs quickly lose the expression of transcription factors associated with pluripotency and self-renewal (Sox-2, Oct-4, and Nanog) and CXCR4, the key receptor responsible for stem cell homing. To enhance their therapeutic potential despite in vitro passages, we examined whether ASCs exhibit superior regenerative capacity by expanding them in monolayers following short-term spheroid formation. Spheroid-derived ASCs retained the expression pattern of cell surface markers and adipogenic/osteogenic differentiation capabilities of ASCs constantly cultured in monolayers. However, spheroid-derived ASCs exhibited higher expansion efficiency with less senescence. Moreover, spheroid-derived ASCs expressed significantly higher levels of pluripotency markers, CXCR4, and angiogenic growth factors. Enhanced in vitro migration, associated with the increased expression of matrix metalloproteinases (MMP-9 and MMP-13), was also observed in spheroid-derived ASCs. The enhanced migration and MMP expression could be inhibited by a CXCR4-specific peptide antagonist, AMD3100. Using a murine model with healing-impaired cutaneous wounds, we observed faster healing and enhanced angiogenesis in the wounds treated with spheroid-derived ASCs. Significantly more cellular engraftment of spheroid-derived ASCs in the cutaneous wound tissue was also noted, with evidence of ASC differentiation toward endothelial and epidermal lineages. These findings suggest that short-term spheroid formation of ASCs before monolayer culture enhances their properties of stemness, angiogenesis, and chemotaxis and thereby increases their regenerative potential for therapeutic use. STEM CELLS TRANSLATIONAL MEDICINE *2013;2:584–594*

INTRODUCTION

Adipose-derived stem cells (ASCs) represent an abundant source of multipotent adult stem cells that are easily obtained from subcutaneous adipose tissue via minimally invasive procedures, such as liposuction [1, 2]. Whereas only 0.001%–0.002% of cells found in bone marrow are mesenchymal stem cells (MSCs), up to 1% of adipose cells are estimated to be stem cells [3]. The abundance and availability of ASCs have made them a promising candidate for stem cell therapies in many fields of regenerative medicine. The expression of pluripotency markers, such as Oct4 and Nanog, in MSCs has been shown to increase their potential for proliferation and differentiation while suppressing spontaneous differentiation [4]. Hence, MSC expansion, without loss of self-renewal capacity or differentiation potential, is essential for the successful clinical application of these cells [5]. Human MSCs are

commonly cultured as monolayers using conventional tissue culture techniques, but several reports have demonstrated that in culture, such methods exhibit deteriorating replication, decreased colony-forming efficiency, and decreased expression of pluripotency markers over time [6, 7]. Moreover, the loss of the chemokine response during in vitro culture results in homing impairment and represents a substantial challenge for therapeutic application of ASCs [8]. CXCR4 and its ligand, stromal cell-derived factor-1 (SDF-1), are believed to be key players in the transport of MSCs to injury sites and in the migration of MSCs in vitro [9]. However, MSC homing capabilities are greatly influenced by cell culture conditions. As with the expression of pluripotency markers, only early passages of MSCs express CXCR4 and chemotactically respond to SDF-1 [10].

Despite the abundance of ASCs that are present in adipose tissue, culture-expanded ASCs are

required for many clinical applications [11]. Therefore, maintaining the expression of stemness markers and of CXCR4 during in vitro expansion of ASCs has become an important issue. Attempts to increase MSC stemness include forcing the expression of Nanog or Sox2 defined genes [12] and treating cells with growth factors such as bone morphogenetic protein 4 [13]. Enhanced functional CXCR4 expression in ASCs involves transduction of MSCs with a retroviral vector encoding for CXCR4 [8] and treatment of the cells with insulin-like growth factor [14]. However, these maneuvers, involving genetic transfection and chemical stimulation, may also adversely affect the cells and thus create safety concerns for clinical use.

In contrast to monolayer culture, culturing MSCs as three-dimensional (3D) aggregates causes substantial changes in the pattern of gene expression [15–17]. We previously reported formation of spheroid human ASCs with upregulated pluripotency genes, including *Oct4*, *Sox2*, and *Nanog*, on chitosan films. Moreover, ASCs within these spheroids were more resilient in serum-free culture conditions. In a nude mouse model, we found that transplantation of ASC spheroids in place of dissociated cells increases cellular retention rates [18]. These findings are in line with other reports that identify aggregation of mesenchymal stem cells as a procedure to enhance their therapeutic potential, including anti-inflammation, angiogenesis, and homing to injury sites [15–17]. Although the use of 3D spheroid culture methods holds promise in the field of cell therapy, it is not clear whether the cells within spheroids can retain their regenerative capabilities if the 3D culture environment is disrupted by further cell expansion in monolayers.

This study aimed to develop a straightforward and effective method of biomaterial-mediated short-term spheroid formation to increase the regenerative capabilities of ASCs for clinical application. Our results show that ASCs within spheroids can be further expanded in monolayer culture and exhibit superior biological properties in terms of stemness, angiogenesis, and chemotaxis. Moreover, administration of expanded spheroid-derived ASCs in a murine model of impaired cutaneous wound healing enhanced tissue regeneration as compared with treatment with cells derived from constant monolayer culture.

MATERIALS AND METHODS

Cell Harvest and Cell Culture

Primary ASCs were isolated by abdominoplasty from five female donors with an average age of 42 years (range, 30–57 years) and an average body mass index of 24.8 kg/m^2 (range, 21.0–26.6 kg/m^2). The study protocol was approved by the Internal Ethical Committee of National Taiwan University Hospital. The adipose tissue was placed in a physiological solution (0.9% NaCl), washed twice with phosphate-buffered saline (PBS; Omics Biotechnology, Taipei, Taiwan, http://www.omicsbio.com.tw), and finely minced. The scraped adipose tissue was then digested with 1 mg/ml collagenase type I (Gibco, Carlsbad, CA, http://www.invitrogen.com) solution at 37°C in agitation for 60 minutes. The cells were expanded on tissue culture polystyrene (TCPS; Greiner Bio-One, Frickenhausen, Germany, http://www.greinerbioone.com) in medium consisting of Dulbecco's Modified Eagle's Medium: Nutrient Mixture F-12 (DMEM/F12) (HyClone, Logan, UT, http://www.hyclone.com), 10% fetal bovine serum (FBS; Biological Industries, Kibbutz Beit Haemek, Israel, http://www.bioind.

com), 1% antibiotic-antimycotic (Biological Industries), and 1 ng/ml fibroblast growth factor-2 (FGF-2; R&D Systems Inc., Minneapolis, MN, http://www.rndsystems.com). Third-passage ASCs were plated onto chitosan film at a density of 2.50 × 10^4 cells per cm^2 using a previously described method [18]. The culture medium consisted of DMEM-high glucose (HG; Gibco), 10% FBS, and 1% antibiotic-antimycotic. The culture medium was refreshed every 2–3 days. After 7 days of culture, ASC spheroids formed on chitosan films were dissociated by repeated pipetting in HyQtase (HyClone) solution, transferred to new TCPS, and expanded for 7 more days before cell harvest for further experiments (spheroid-derived ASCs). We used ASCs that were constantly cultured on TCPS as the control (monolayer ASCs).

Flow Cytometry Analysis

To determine cell surface antigen expression, the ASC samples were incubated with the following antibodies: human monoclonal antibodies against CXCR4 (Abcam, Cambridge, MA, http://www.abcam.com), CD31 (BD Pharmingen, San Diego, CA, http://www.bdbiosciences.com), CD34, CD44, CD73, CD90 (all from BioLegend, San Diego, CA, http://www.biolegend.com), CD105 (eBioscience, San Diego, CA, http://www.ebioscience.com), and CD166 (BioLegend). The samples were analyzed using a flow cytometer (FACScan; Becton, Dickinson and Company, Franklin Lakes, NJ, http://www.bd.com). Positive cells were determined as the proportion of the population with fluorescence greater than 95% of the isotype control. For apoptosis assay, after exposure to 300 μM H$_2$O$_2$ for 3 hours, spheroid-derived and monolayer ASCs were stained using an Annexin V-fluorescein isothiocyanate apoptosis detection kit (Strongbiotech, Taipei, Taiwan, http://www.strongbiotech.com) according to the supplier's instructions. Cells were analyzed on a flow cytometer and gated according to forward scatter, side scatter, and their ability to exclude propidium iodide (PI). Annexin V-negative and PI-negative cells were considered survival cells.

Differentiation of Human ASCs

Adipogenic differentiation was induced in DMEM-HG supplemented with 10% FBS, 1% antibiotic-antimycotic, 500 μM 3-isobutyl-1-methylxanthine (Sigma-Aldrich, St. Louis, MO, http://www.sigmaaldrich.com), 1 μM dexamethasone (Sigma-Aldrich), 10 μM insulin (Sigma-Aldrich), and 400 μM indomethacin (Sigma-Aldrich). After 7 days, the expression of an adipogenic representative gene, *PPAR-γ*, was analyzed by real-time polymerase chain reaction (PCR). Monolayer and spheroid-derived cells were also fixed in 4% paraformaldehyde and stained with Oil Red O (Sigma-Aldrich) to observe lipid droplets. Osteogenic differentiation was induced by culturing ASC populations in DMEM-HG supplemented with 10% FBS, 1% antibiotic-antimycotic, 10 nM dexamethasone, 50 μM ascorbic acid 2-phosphate (Sigma-Aldrich), 10 nM 1α,25-dihydroxyvitamin D$_3$ (Sigma-Aldrich), and 10 mM β-glycerophosphate (Sigma-Aldrich). At day 7, the expression of an osteogenic representative gene, *Runx2*, was analyzed by real-time PCR. Monolayer and spheroid-derived ASCs were fixed in 4% paraformaldehyde and stained with alizarin red S (Sigma-Aldrich) to observe mineralized matrix apposition.

Proliferation and Senescence Assay

ASCs derived from monolayer or spheroid cultures were seeded at a density of 1,000 cells per cm^2 on TCPS. Every 7 days, cells
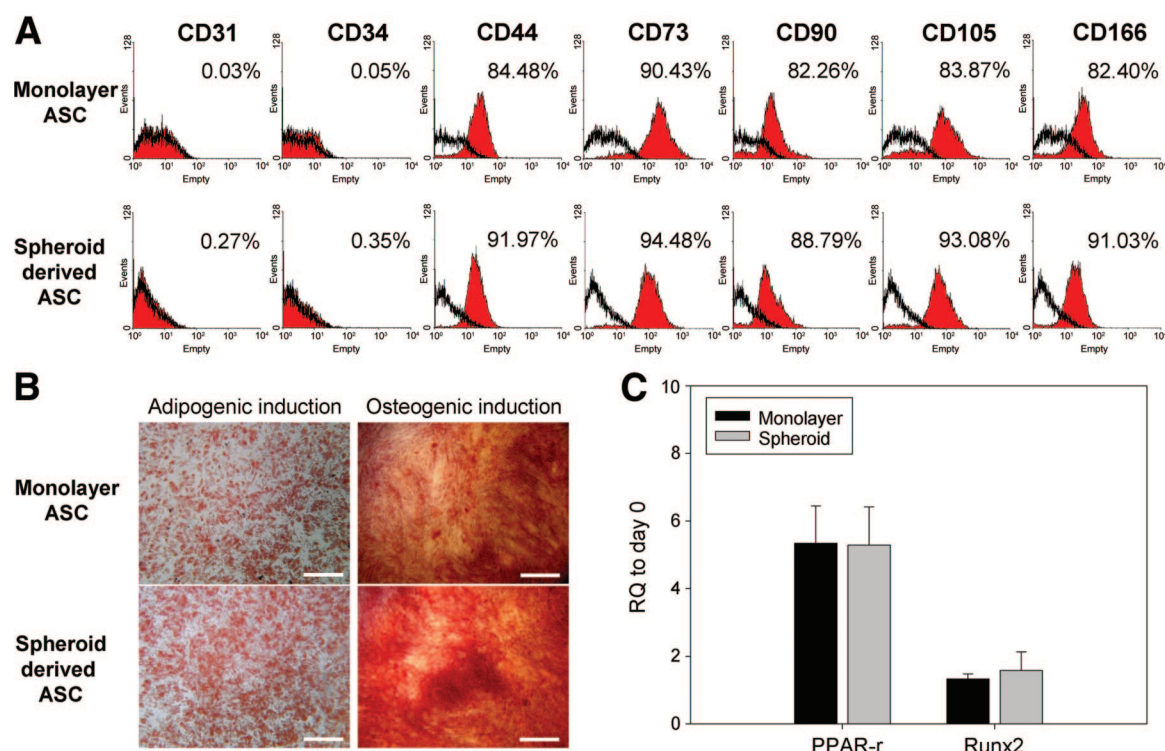
Figure 1. Phenotypic characterization of ASCs derived from spheroid and monolayer cultures. **(A):** The ASCs were plated in monolayer or spheroid cultures for 7 days, followed by replating in monolayer culture for an additional 7 days. The expression level of ASC surface antigens was determined by flow cytometry and is shown as the proportion of positively stained cells relative to an isotype control. **(B):** Microscopic images of monolayer and spheroid-derived ASCs cultured in adipogenic and osteogenic induction media for 14 days. Cell cultures were stained with Oil Red O for detection of adipogenesis and alizarin red for detection of osteogenesis. Scale bars = 100 μm. **(C):** Real-time polymerase chain reaction measurements for adipogenic and osteogenic marker genes ($PPAR$-γ and $Runx2$, respectively) in monolayer and spheroid-derived ASCs at day 7 of induction culture. No significant difference between the monolayer and spheroid-derived cells was noted. Abbreviation: ASC, adipose-derived stem cell.

were lifted, counted, and replated. The process was repeated until cells reached senescence. Moreover, cells were incubated with 5-bromo-2'-deoxyuridine (BrdU) for 24 hours, and BrdU incorporation was then assayed according to the instructions of the cell proliferation enzyme-linked immunosorbent assay (ELISA) kit (Roche, Indianapolis, IN, http://www.roche.com). Cell proliferation was estimated on the basis of the measurement of BrdU incorporation during DNA synthesis in replicating cells.

For evaluation of senescence markers, monolayer and spheroid-derived ASCs were stained with fresh senescence-associated β-galactosidase (SA-β-gal) chromogenic substrate solution. The number of cells stained positive with β-galactosidase was calculated. For determination of lactate dehydrogenase (LDH) released by dead cells into the medium, a cytotoxicity detection kit (Roche) was used at the indicated times by measuring the optical density at 490 nm obtained from an ELISA plate reader (Molecular Devices, Sunnyvale, CA, http://www.moleculardevices.com).

In Vitro Scratch and Chemotaxis Assay

Monolayer and spheroid-derived ASCs were seeded in six-well culture plates (Corning, Lowell, MA, http://www.corning.com), and the well surface was gently scratched with a pipette tip, creating a rectangular cell-free zone. After removal of culture medium and detached cells, remaining cells were washed twice with PBS and cultured for 10 hours. In some wells with spheroid-derived ASC culture, a CXCR4 antagonist, 100 ng/ml AMD3100

(Sigma-Aldrich), was added in the medium. The cell images were photographed under an inverted microscope (Nikon, Tokyo, Japan, http://www.nikon.com), and in vitro migration of cells into a cell-free area was analyzed using ImageJ software.

The migratory ability of monolayer or spheroid-derived ASCs was determined using 8 μm pore size Transwell inserts (Corning). Briefly, ASCs in 100 μl of medium were seeded into the upper well with or without 100 nM AMD3100, and 650 μl of medium with or without 30 ng/ml SDF-1 (Sigma-Aldrich) was placed in the lower well of a 24-well plate. Another group without supplementation of AMD3100 and SDF-1 served as a control. After 6 hours, cell migration through the membrane was assessed by measuring fluorescence in the lower compartment with 4',6-diamidino-2-phenylindole (DAPI; Santa Cruz Biotechnology Inc., Santa Cruz, CA, http://www.scbt.com) staining under a fluorescent microscope (Leica, Heerbrugg, Switzerland, http://www.leica.com).

Reverse Transcription-PCR

Total RNAs of spheroid-derived and monolayer ASCs were extracted with TRIzol reagent (Invitrogen, Carlsbad, CA, http://www.invitrogen.com) according to the manufacturer's instructions. RNA concentration was determined by optical density at 260 nm (OD_{260}) using a spectrophotometer (Nanodrop ND-1000; Thermo Scientific, Waltham, MA, http://www.thermoscientific.com). Once RNA was isolated, complementary DNA (cDNA) was synthesized from RNA using High-Capacity cDNA Reverse Transcription Kits (Applied Biosystems, Foster City, CA, http://www.
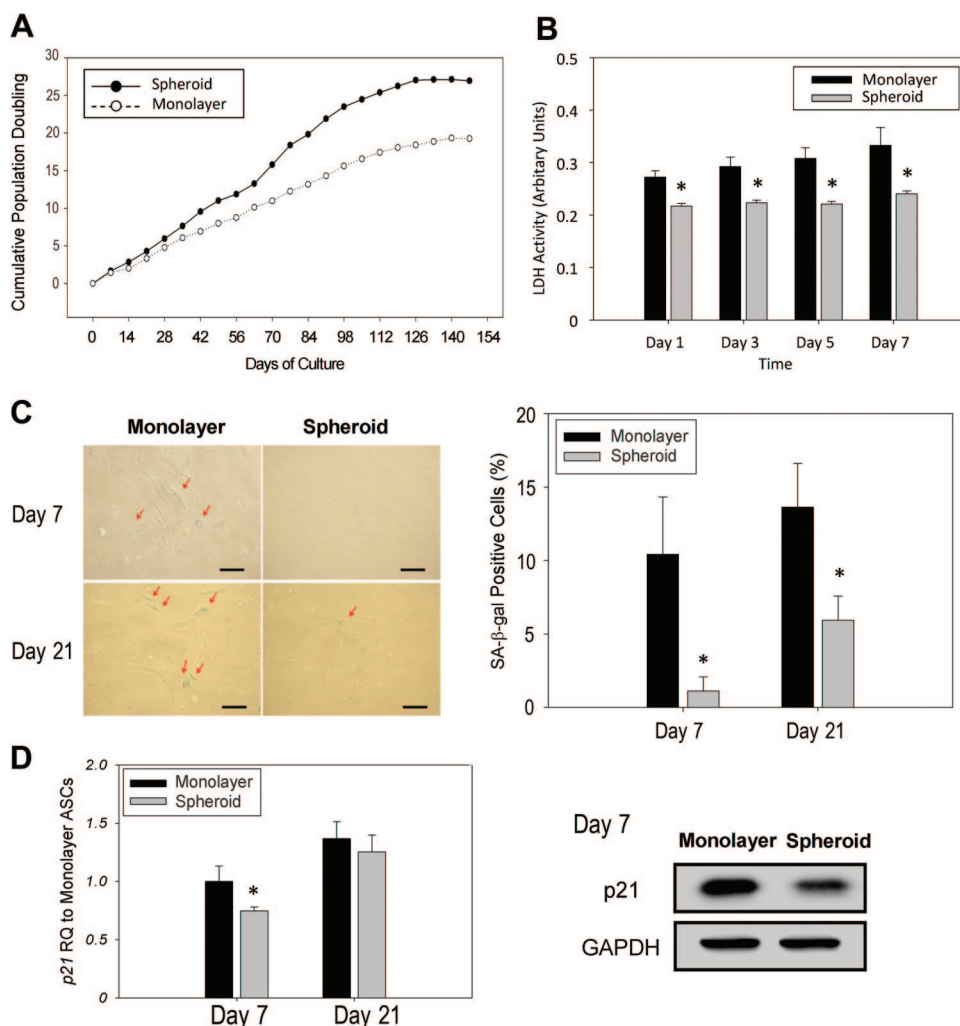
Figure 2. Spheroid-derived ASCs exhibited higher growth rate and lower senescence. **(A):** Cumulative population doubling curve of monolayer and spheroid-derived ASCs. Cells were plated at low density and passaged every 7 days. **(B):** LDH efflux assay of monolayer and spheroid-derived ASCs after serum starvation for 1, 3, 5, and 7 days. At all indicated times during serum starvation, significantly less LDH activity was observed in medium overlying the spheroid-derived ASCs. **(C):** SA-β-gal staining of monolayer and spheroid-derived ASCs after 7 and 21 days of culture revealed significantly more SA-β-gal-positive cells in the monolayer group. Scale bars = 100 μm. **(D):** Real-time polymerase chain reaction and Western blot analysis for senescence marker p21 showed less p21 expression in spheroid-derived ASCs on day 7. ∗, $p < .05$ versus the monolayer condition at the same time point. Abbreviations: ASC, adipose-derived stem cell; LDH, lactate dehydrogenase; SA-β-gal, senescence-associated β-galactosidase; RQ, relative quantity.

appliedbiosystems.com). The sequences of the gene-specific primers are shown in supplemental online Table 1. Briefly, quantitative reverse transcription-PCR was performed in triplicate using a StepOne Real-Time PCR system (Applied Biosystems). The expression level was analyzed and normalized to glyceraldehyde-3-phosphate dehydrogenase (GAPDH) for each cDNA sample. Relative quantity of gene expression was calculated with comparative C_T method.

Quantifying Secreted Hepatocyte Growth Factor

Conditioned media of monolayer and spheroid-derived ASCs for 48 hours were analyzed using an ELISA kit for human hepatocyte growth factor (HGF; Quantikine; R&D Systems). Data were expressed as the secreted factor per 10^5 cells at the time of harvest.

Western Blot

The protein expression was determined at day 7 of cell culture. Monolayer and spheroid-derived ASCs were resuspended in cell ly-

sis buffer and sonicated. After centrifugation, the protein content was determined in the supernatants by a bicinchoninic acid protein quantification kit (Pierce, Rockford, IL, http://www.piercenet.com). Sixty micrograms of proteins from spheroids or monolayer cells was added to Laemmli sample buffer and boiled for 10 minutes. Proteins were separated by sodium dodecyl sulfate-polyacrylamide gel electrophoresis and blotted onto polyvinylidene difluoride membranes. Western blot was performed using anti-p21 (Cell Signaling Technology, Danvers, MA, http://www.cellsignal.com), anti-matrix metalloproteinase (MMP)-9, and anti-MMP-13 (both from Epitomics, Burlingame, CA, http://www.epitomics.com), anti-Oct4 (Genetex, Irvine, CA, http://www.genetex.com), anti-Sox2, anti-Nanog (both from R&D Systems), anti-CXCR4 (Abcam), anti-vascular endothelial growth factor (VEGF; Epitomics), anti-HGF (Santa Cruz Biotechnology), and anti-GAPDH (Epitomics). The membranes were incubated with the primary antibodies overnight at 4°C. After extensive washing, the membranes were further incubated with horseradish peroxidase-conjugated secondary antibodies for 1

hour. The blots were then developed using an enhanced chemiluminescence detection system (Millipore, Billerica, MA, http://www.millipore.com).

In Vivo Wound Healing Model

At least four female nude mice (20–25 g body weight; National Laboratory Animal Center, Taipei, Taiwan) were used per condition, in accordance with the animal care guidelines of National Taiwan University. On the day of surgery, two 9-mm round full-thickness cutaneous wounds were created on each side of the dorsal midline. Immediately after wounding, mitomycin C solution (1 mg/ml) was applied for 10 minutes to create a healing-impaired wound [19]. Cultured monolayer or spheroid-derived ASCs (7.5×10^5 cells) in 100 μl of PBS were then subcutaneously injected around the dorsal wound. The contralateral wound was injected with PBS only. Wounds were circumscribed with donut-shaped silicone splints held in place using 6-0 nylon sutures to prevent wound contraction, and then covered with a transparent, semiocclusive adhesive dressing (Tegaderm; 3M, St. Paul, MN, http://www.3m.com). Digital photographs of the wounds were taken regularly, and the wound size was estimated using planimetric methods (ImageJ).

Histomorphometric Examination and Immunofluorescence

On postoperative days 7 and 14, the cutaneous wounds were harvested, including 0.5 cm of the surrounding skin area. Tissue specimens were cut in the midline. One piece was snap frozen in liquid nitrogen. The remaining piece was fixed in 10% formalin solution for paraffin-embedded histological analysis. Sections were cut perpendicular to the anterior-posterior axis and perpendicular to the surface of the wound. Paraffin-embedded sections were rehydrated and stained with hematoxylin and eosin (Sigma-Aldrich). Sections close to the center of the wounds were selected for determination of the area of granulated tissue by ImageJ software. Frozen sections were fixed with acetone and stained with human nuclear antigen (HNA; Millipore) to detect transplanted human cells. To determine the proliferation of capillaries in wounds, sections were subjected to immunofluorescent staining with anti-CD31. Frozen sections were stained with anti-Ki-67 (Abcam) to detect keratinocyte proliferation, and pancytokeratin (Abcam) for detecting epidermal cells. To quantify immunolabeled cells, DAPI counterstaining was performed, and 10 different images per slide from three different samples were randomly analyzed.

Statistical Analysis

All measurements are presented as means $\pm$ SD. Statistical significance was evaluated using an independent-samples Student's t test or analysis of variance, followed by Scheffé's post hoc test. All statistical analyses were performed using STATA software (StataCorp, College Station, TX, http://www.stata.com). Statistically significant values were defined as $p < .05$.

RESULTS

Characterization of Spheroid-Derived ASCs

Spheroid formation was noted as human ASCs were cultured on chitosan films for 7 days [18]. ASCs dissociated from 7-day-old spheroids were further cultured on TCPS in monolayers for 7 days. The surface epitopes of these spheroid-derived ASCs were similar to those of ASCs harvested from monolayer cultures with-
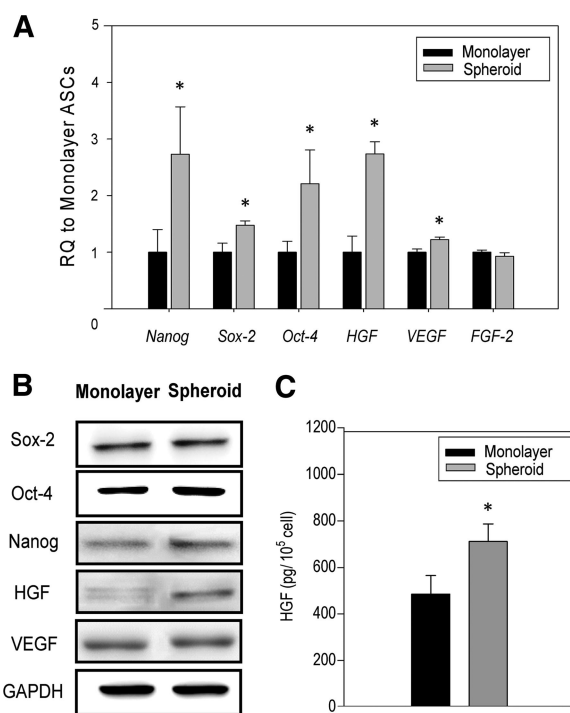

Figure 3. Expression of stemness markers and angiogenic growth factors in spheroid-derived ASCs. **(A):** Real-time polymerase chain reaction measurements for pluripotency marker genes (*Nanog*, *Sox-2*, and *Oct-4*) and angiogenic growth factors (*HGF*, *VEGF*, and *FGF-2*) in monolayer and spheroid-derived ASCs. **(B):** Western blot analysis of the expression of pluripotency markers and angiogenic growth factors in monolayer and spheroid-derived ASCs. **(C):** Release of HGF from monolayer and spheroid-derived ASCs into the media as determined by enzyme-linked immunosorbent assay. $*, p < .05$ versus the monolayer condition. Abbreviations: ASC, adipose-derived stem cell; FGF-2, fibroblast growth factor-2; HGF, hepatocyte growth factor; RQ, relative quantity; VEGF, vascular endothelial growth factor.

out previous experience of spheroid formation (monolayer ASCs). These ASCs were negative for hematopoietic markers CD31 and CD34 and were positive for MSC-related markers CD44, CD73, CD90, CD105, and CD166 (Fig. 1A). Moreover, spheroid-derived ASCs maintained their adipogenic and osteogenic differentiation capabilities after application of appropriate induction media, as demonstrated by histology staining specific for oil and calcium, respectively (Fig. 1B). Determination of relative gene expression levels by real-time PCR after adipogenic or osteogenic induction showed no significant difference in transcription levels for *PPAR-γ* or *Runx2* between spheroid-derived and monolayer ASCs (Fig. 1C).

Spheroid-derived ASCs expanded more rapidly through passages compared with monolayer ASCs before reaching senescence at roughly the same time point after initial seeding (Fig. 2A). LDH efflux assay revealed less cell death due to senescence for spheroid-derived ASCs in a serum-free culture condition (Fig. 2B). In comparison with monolayer cells, senescence, as assayed by SA-β-gal staining, was also significantly decreased in spheroid-derived ASCs after 7 or 21 days of culture (Fig. 2C). However, p21 protein, which is highly expressed in senescent cells, was significantly downregulated in spheroid-derived ASCs on day 7, but not day 21 (Fig. 2D).
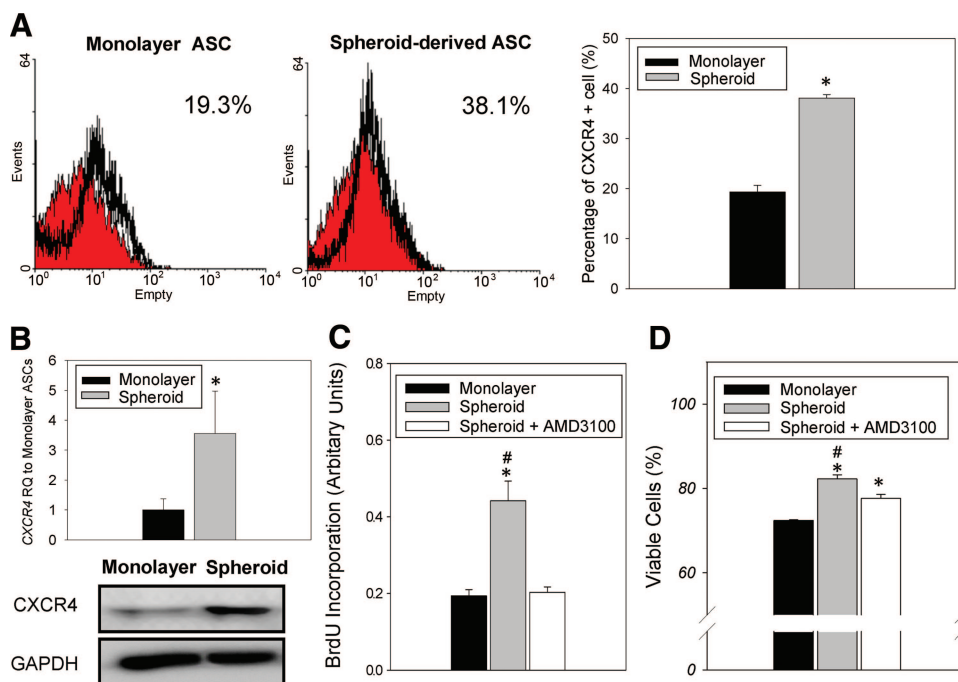
Figure 4. Enhanced CXCR4 expression in spheroid-derived ASCs. **(A):** Flow cytometric analysis of a stem cell homing marker, CXCR4, revealed significantly more CXCR4-positive cells in ASCs that had experienced spheroid cultures. **(B):** Real-time polymerase chain reaction and Western blot analysis showed higher CXCR4 expression in spheroid-derived ASCs compared with monolayer cells. **(C):** Monolayer and spheroid-derived ASCs were incorporated with BrdU for 24 hours and then detected by enzyme-linked immunosorbent assay, which indicated proliferative activity. The significant increase of BrdU incorporation in spheroid-derived ASCs could be reversed by adding a CXCR4 antagonist, AMD3100. **(D):** The percentages of viable monolayer and spheroid-derived ASCs after exposure to H_2O_2 were determined by flow cytometry measuring propidium iodide uptake and annexin V-fluorescein isothiocyanate labeling. The ratio of survival cells was significantly higher in the group that had undergone short-term spheroid culture, and the ratio decreased after addition of AMD3100. ∗, $p < .05$ versus the monolayer condition; #, $p < .05$ versus the spheroid + AMD3100 condition. Abbreviations: ASC, adipose-derived stem cell; BrdU, 5-bromo-2′-deoxyuridine; GAPDH, glyceraldehyde-3-phosphate dehydrogenase; RQ, relative quantity.

Spheroid Formation Increased the Expression of Pluripotent Markers, Angiogenic Growth Factors, and CXCR4

The relative mRNA expression of pluripotency-associated transcription factors Nanog, Sox2, and Oct4 and angiogenic growth factors, including HGF, FGF-2, and VEGF, was analyzed by real-time PCR. Spheroid-derived ASCs exhibited significantly greater expression levels of *Nanog*, *Sox2*, and *Oct4* with 2.7 ± 0.8-fold, 1.5 ± 0.1-fold, and 2.2 ± 0.6-fold increases, respectively, compared with monolayer ASCs. The *HGF* and *VEGF* transcription numbers were also greater in the spheroid-derived ASCs, with 2.7 ± 0.2-fold and 1.2 ± 0.1-fold increases, respectively, over those of monolayer ASCs. There was no significant difference in *FGF-2* gene expression between the two groups (Fig. 3A). Western blot analysis also showed greater Sox2, Oct4, Nanog, HGF, and VEGF expression in spheroid-derived ASCs than for monolayer ASCs (Fig. 3B). ELISA analysis of HGF levels in human ASC supernatants further confirmed the significantly greater expression of HGF in spheroid-derived ASCs (Fig. 3C).

Flow cytometry revealed that 38.1 ± 0.7% of spheroid-derived ASCs were positive for the MSC homing receptor CXCR4, and this ratio was significantly greater than that for monolayer ASCs at 19.3 ± 1.3% (Fig. 4A). Real-time PCR and Western blot analysis also showed elevated CXCR4 expression in spheroid-derived ASCs (Fig. 4B). BrdU incorporation assay revealed significantly enhanced proliferation in spheroid-derived ASCs, and we found that adding the CXCR4 antagonist, AMD3100, decreased BrdU incorporation to levels comparable to those of monolayer ASCs (Fig. 4C). We used flow cytometry to examine cellular apo-

ptosis/necrosis in spheroid-derived and monolayer ASCs after exposure to H_2O_2. The survival ratio of spheroid-derived ASCs was significantly higher relative to monolayer ASCs, and it decreased after treatment with AMD3100 (Fig. 4D).

Spheroid-Derived ASCs Exhibit Enhanced Chemotactic Response In Vitro

Spheroid-derived ASCs exhibited significantly increased *MMP-9* and *MMP-13* gene expression, with estimated 3.9 ± 0.3 and 6.6 ± 2.0-fold increases, respectively, compared with those for the monolayer ASCs. Addition of AMD3100 to the culture medium inhibited the enhancement in MMP expression, and this finding was confirmed by Western blot analysis (Fig. 5A). Both spheroid-derived and monolayer ASCs were subjected to in vitro cell migration assay by scratching confluent cells with a pipette tip and completely removing the resulting debris by repeated washing. After 10 hours, images of cells were analyzed; we noted that migrated cells in the spheroid-derived group had covered a significantly larger area (80.3 ± 5.8%) compared with the monolayer ASCs (60.5 ± 5.7%). Supplementing the culture medium with AMD3100 revealed a reduction in the cell coverage area of the spheroid-derived ASCs to 71.5 ± 0.6% (Fig. 5B). Spheroid-derived and monolayer ASCs were also subjected to Transwell chemotaxis assay toward the CXCR4 ligand, SDF-1. Even without adding SDF-1 to the lower wells, we found significantly more migrated cells in the spheroid-derived group, with a 2.9 ± 0.2-fold increase relative to the monolayer group. The migrated cell number for spheroid-derived ASCs showed a significant 5.1 ±
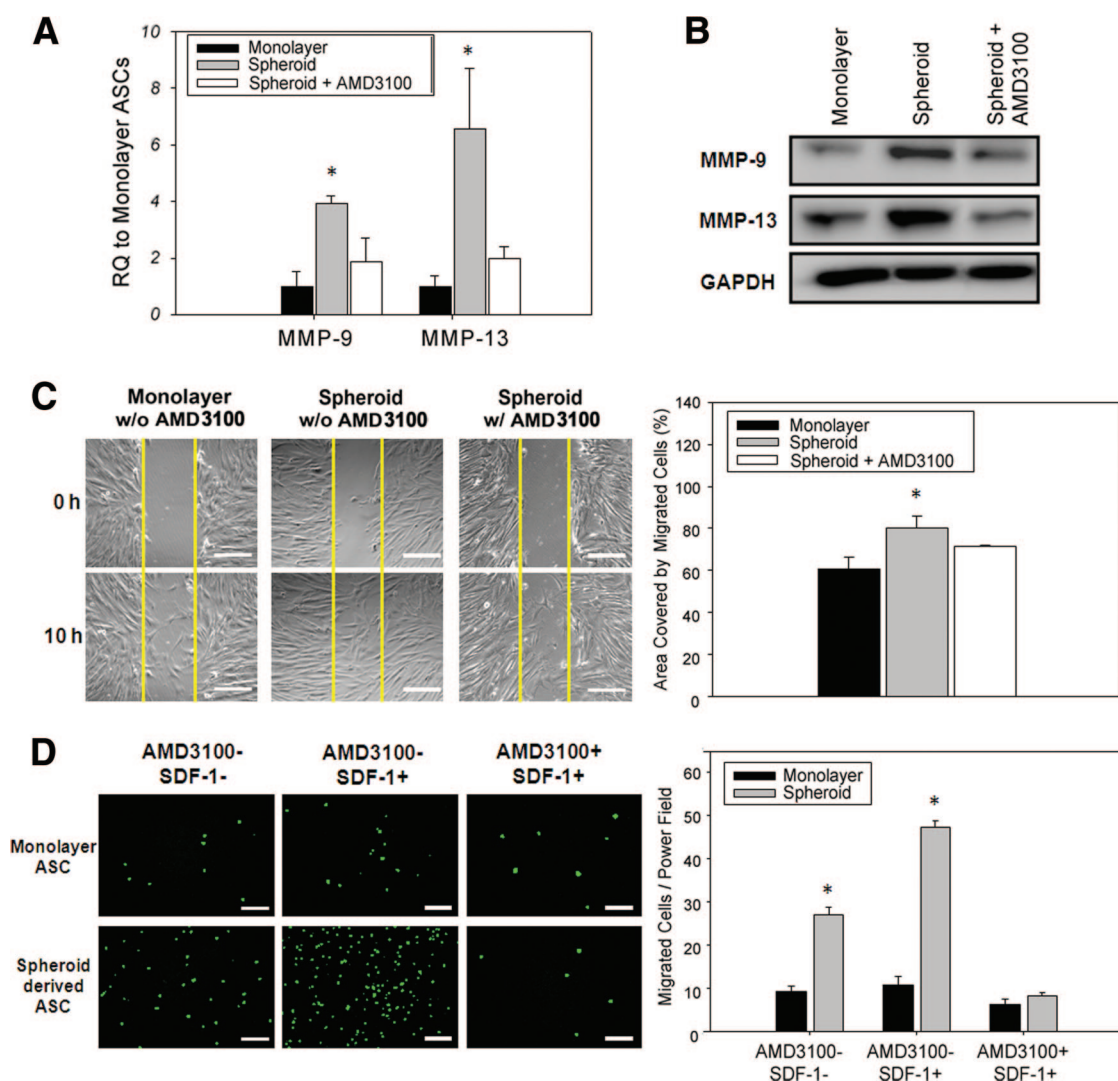
Figure 5. Enhanced MMP expression and chemotaxis in spheroid-derived ASCs were associated with CXCR4 upregulation. **(A, B):** Real-time-polymerase chain reaction **(A)** and Western blot analysis **(B)** for MMP-9 and MMP-13 expression revealed significantly higher MMP-9 and MMP-13 expression in spheroid-derived ASCs compared with monolayer cells, and the enhanced expression was inhibited by adding a CXCR4 antagonist, AMD3100. *, $p < .05$ versus other conditions for each MMP. **(C):** In vitro cell migration was evaluated by scratching confluent ASCs with a pipette tip. After 10 hours, the area of the cell-free zone covered by the migrated cells was measured. *, $p < .05$ versus the monolayer condition. **(D):** Chemotactic assay evaluated ASC migration through 8 μm pore size Transwell inserts toward SDF-1. Cells were stained with DAPI (green). Enhanced migration and chemotaxis of spheroid-derived ASCs compared with monolayer cells could be inhibited by supplementing with AMD3100. Scale bars = 50 μm. *, $p < .05$ versus all other conditions. Abbreviations: ASC, adipose-derived stem cell; DAPI, 4′,6-diamidino-2-phenylindole; MMP, matrix metalloproteinase; RQ, relative quantity; SDF, stromal cell-derived factor; w, with; w/o, without.

0.2-fold increase if the lower well was supplemented with SDF-1, whereas no significant difference was seen in the monolayer group despite supplementation with SDF-1. The enhanced chemotaxis of spheroid-derived ASCs toward SDF-1 was eliminated by adding AMD3100 to the culture medium (Fig. 5C).

Tissue Regeneration Is Enhanced in Skin Defects Seeded With Spheroid-Derived ASCs via Angiogenesis and Differentiation

To assess the regenerative capability of spheroid-derived ASCs in vivo, we used a murine model with impaired cutaneous wound healing induced by topical treatment with mitomycin [19]. Treating the wounds with spheroid-derived ASCs resulted in a significantly smaller wound area by postwounding day 10 compared with treatment with monolayer ASCs or PBS (Fig. 6A). The histol-

ogy of the wound sections showed a significantly greater area of granulated tissue in wounds treated with spheroid-derived ASCs (Fig. 6B). Moreover, significantly more proliferative marker Ki-67-labeled cells were present in wound sections treated with spheroid-derived ASCs (supplemental online Fig. 1).

To further investigate ASC engraftment and angiogenesis, we performed immunofluorescent staining of HNA and CD31 in wound sections at postwounding days 7 and 14 (Fig. 7A). Wounds treated with spheroid-derived ASCs exhibited a significantly greater number of transplanted ASCs (HNA-positive cells) compared with the monolayer group (7.8 ± 2.6 ASCs per high-power field vs. 3.0 ± 1.0 on day 7; 4.7 ± 1.1 ASCs per high-power field vs. 1.4 ± 1.3 on day 14, $p < .05$). The numbers of CD31-stained capillaries in wound sections were also significantly increased in wounds treated with
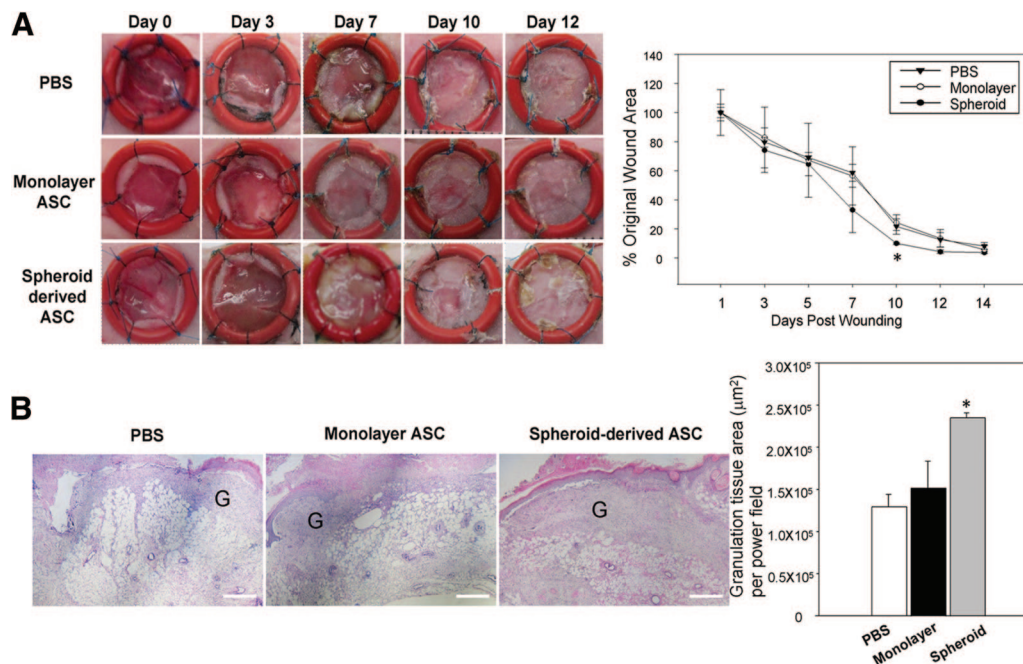
Figure 6. Delivery of spheroid-derived ASCs enhanced cutaneous wound closure. **(A):** Gross pictures and wound area curves show accelerated healing in wounds treated with spheroid-derived ASCs. **(B):** Hematoxylin and eosin staining of wound sections at day 7. A significantly larger area of granulation tissue was observed in wounds treated with spheroid-derived ASCs. Scale bars = 200 μm. *, $p < .05$ versus the other two groups. Abbreviations: ASC, adipose-derived stem cell; G, granulation tissue; PBS, phosphate-buffered saline.

spheroid-derived ASCs compared with those treated with monolayer ASCs (163 ± 30 vs. 71 ± 24 vessels per mm^2 on day 7; 166 ± 41 vs. 101 ± 13 vessels per mm^2 on day 14, $p < .05$). No significant difference in capillary densities was noted between wounds treated with monolayer ASCs and PBS (Fig. 7B). Moreover, colocalization of HNA with two cell lineage-specific markers was observed in wound sections to assess ASC differentiation in vivo. Colocalization of HNA and CD31 immunofluorescence was more prominent in wounds treated with spheroid-derived ASCs than in those treated with monolayer ASCs, suggesting that transplanted ASCs differentiate toward the endothelial lineage. HNA-positive cells were also found to colocalize with pancytokeratin immunofluorescence in wound sections that had received spheroid-derived ASC treatment, indicating that spheroid-derived ASCs contribute to the regeneration of epidermal structures. Such HNA and pancytokeratin colocalization was not seen in wounds treated with monolayer ASCs (Fig. 7C). Higher magnification images of HNA, CD31, and pancytokeratin immunofluorescence on day 14 wound sections are given in supplemental online Figure 2.

DISCUSSION

The 3D culture methods resulted in improved cell-cell contacts with greater interactions between cells and the extracellular matrix than conventional culture methods afford, thus creating cellular environments close to in vivo conditions. Significant differences in biological responses and cellular phenotypes are seen between monolayer and 3D cell culture [16, 18, 20]. In the present study, we further showed that the regenerative capacity of ASCs is enhanced after short-term spheroid formation on chitosan films, despite further expansion by monolayer cultures. Spheroid-derived ASCs exhibited greater expression of pluripo-

tency markers Sox-2, Oct-4, and Nanog compared with ASCs that were constantly cultured in monolayers. Therefore, the stemness of ASCs was maintained, even though the cells were no longer in the niche environment of a spheroid. Moreover, spheroid-derived ASCs exhibited higher proliferative activity. Although ASCs cease to proliferate upon spheroid formation, later expansion of dissociated spheroid cells in monolayers can yield additional progeny for therapeutic use.

We evaluated the senescence markers, including SA-β-gal staining and p21 expression, of monolayer and spheroid-derived ASCs after 7 and 21 days of culture. Significantly more SA-β-gal-positive cells in the monolayer group were noted at both time points. However, real-time PCR revealed significant downregulation of p21 in spheroid-derived ASCs on day 7, but not day 21. The data suggested that the effect of short-term spheroid culture gradually deteriorated, but it did not completely disappear after 21 days of adherent culture. Moreover, spheroid-derived ASCs also experienced lower senescence in a serum-free culture environment as measured by LDH assay, which may indicate greater survival advantages in hazardous environments for these cells. Consequently, our animal experiment demonstrated improved cellular retention if spheroid-derived ASCs were injected into cutaneous wounds compared with a significantly lower retention rate resulting from administration of ASCs constantly cultured in monolayers.

Culturing ASCs in cellular aggregates has been shown to enhance the secretion of angiogenic growth factors as compared with monolayer cultures [16]. In this study, we found that after further expansion of spheroid-derived ASCs in monolayers, there was significant upregulation of *VEGF* and *HGF*, but not *FGF-2*. In particular, spheroid-derived ASCs exhibited an average 2.7-fold increase in *HGF* gene transcripts relative to monolayer ASCs. ELISA also revealed a significantly greater HGF concentration in
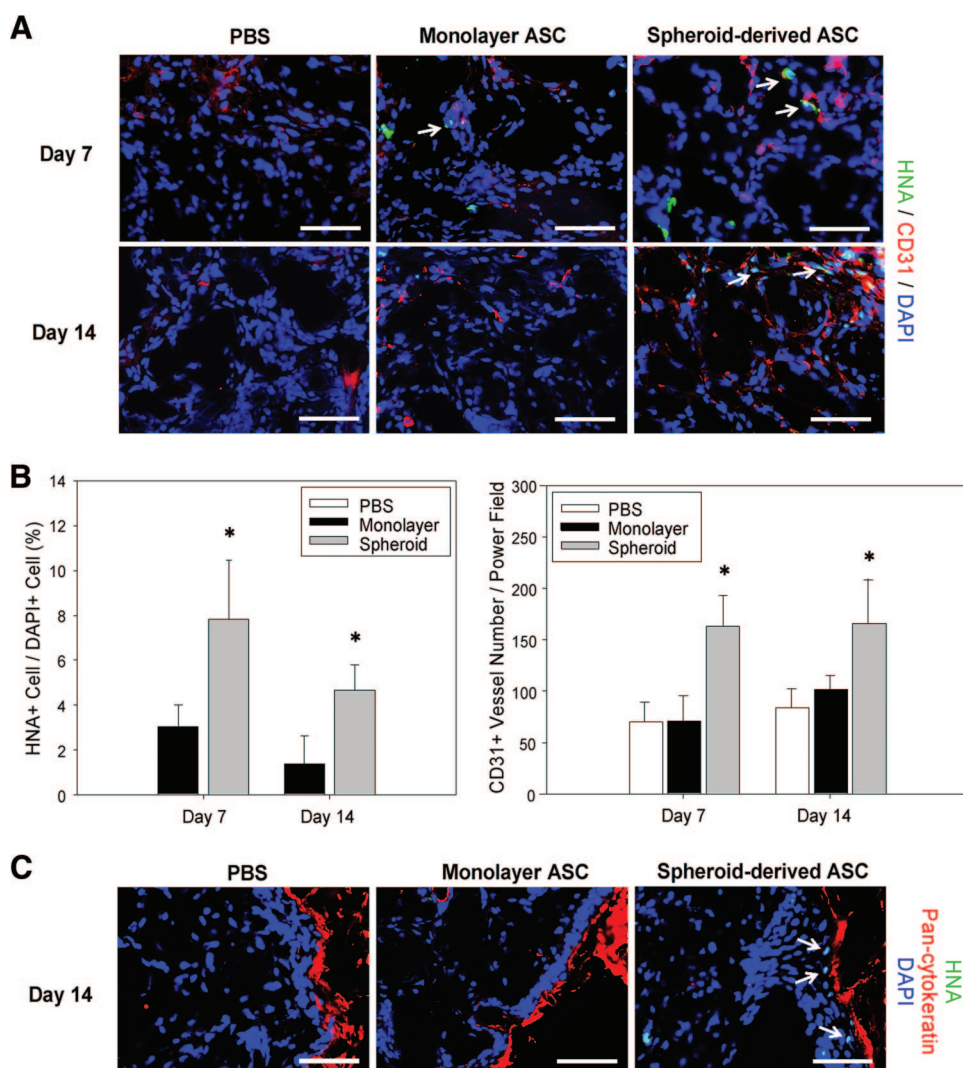
Figure 7. Enhanced cell engraftment and angiogenesis in wounds treated with spheroid-derived ASCs. **(A):** Double immunofluorescent staining of HNA and an endothelial marker, CD31. White arrows indicate human ASCs incorporated into vasculature. **(B):** The ratio of HNA-positive cells was significantly higher in the spheroid group, suggesting a higher ASC retention rate at both day 7 and day 14. Quantification of capillary density per high-power field also revealed significantly enhanced angiogenesis in wounds treated with spheroid-derived ASCs. The numbers of capillary and HNA-positive cells were calculated from 10 randomly selected high-power fields per sample. **(C):** Double immunofluorescent staining of HNA and an epithelial marker, pancytokeratin. White arrows indicate human ASCs incorporated into the epidermal structure. Cells were counterstained with DAPI (blue). Scale bars = 50 μm. *, $p < .05$ versus other groups at the same time point. Abbreviations: ASC, adipose-derived stem cell; DAPI, 4′,6-diamidino-2-phenylindole; HNA, human nuclear antigen; PBS, phosphate-buffered saline.

the spheroid-derived ASC culture medium. It has been shown that HGF production is important for ASC potency and that HGF mediates the proangiogenic, prosurvival, and repair promotion activities of ASCs [21]. These in vitro findings are in agreement with our in vivo results, indicating that wounds treated with spheroid-derived ASCs exhibit significantly greater ASC retention and capillary density than monolayer ASCs do.

SDF-1-mediated CXCR4 signaling plays important roles in the migration, engraftment, and proliferation of stem cells. Cytokine SDF-1 is released in response to hypoxia and acts as a chemoattracting factor, recruiting CXCR4-expressing cells to sites of ischemia or injury [22]. MSCs lose their CXCR4 expression shortly after isolation, and only a small portion of culture-expanded MSCs are CXCR4-positive [9, 23, 24]. Culturing MSCs as 3D aggregates can restore functional CXCR4 expression and consequently regulates MSC adhesion to endothelial cells [9]. In this study, we

found that *CXCR4* remained significantly upregulated in monolayer culture-expanded spheroid-derived ASCs. AMD3100, an antagonist of CXCR4, inhibited the enhanced mitotic activity and the reduced apoptosis and necrosis seen in spheroid-derived ASCs upon exposure to H_2O_2. Moreover, increased in vitro migration of spheroid-derived ASCs along an SDF-1 concentration gradient, accompanied by enhanced production of MMP-9 and MMP-13, were also partially inhibited by AMD3100. It has been shown that CXCR4 overexpression, induced by retroviral transduction in ASCs, showed enhanced migration and tissue engraftment [8, 25]. The upregulation of MMP-9 in MSCs that overexpress CXCR4 is responsible for enhanced cellular invasion via the basement membrane and for improved remodeling of ischemic heart tissue [26]. This report demonstrates that a short period of spheroid formation can enhance the functional expression of CXCR4 in ASCs, circumventing the safety issue regarding

gene transfection, and so is a more practical technique for clinical application of CXCR4-positive ASCs.

The molecular processes that increase the expression of pluripotent markers, angiogenic growth factors, and CXCR4 in spheroid-derived ASCs are unclear. Previous studies have shown a high cellular survival rate of MSCs within spheroids [17, 18]; thus, it is less likely that the enhanced stemness that occurs after short-term spheroid formation results from a selection process whereby MSCs with lower stemness markers are eliminated. One obvious change upon spheroid ASC formation is the development of a hypoxic environment in the core of each spheroid [18, 27]. Hypoxic MSC culturing conditions prevent replicative senescence and enhance proliferation capacity and lifespan; consequently, stem cell properties are maintained [5]. Moreover, hypoxia-treated ASCs stimulate angiogenesis and maturation of newly formed blood vessels in vivo [28]. Restricting the oxygen supply to MSCs for short periods can increase their CXCR4 expression and in vivo engraftment [29]. Therefore, hypoxia preconditioning may be a contributing factor to the therapeutic potential of spheroid-derived ASCs. However, cellular spheroid formation also provides certain characteristics other than hypoxia, such as a rounded cell morphology and increased cell-cell contact area [18]. In particular, the biomaterial-mediated ASC spheroid formation was suggested to own unique substrate-dependent properties, rendering them different from those generated by suspension or hanging drops [17]. Spheroid formation on chitosan films requires no specialized culture facilities, such as a hypoxic chamber, and thus provides a useful and accessible technique to enhance the regenerative capacity of ASCs during in vitro culture.

Transplantation of MSCs formulated as multicellular aggregates provides enhanced cellular engraftment compared with that offered by dissociated MSCs [18, 27]. In a diabetic mouse model, ASC spheroid-treated wounds exhibited significant increases in wound closure rate compared with wounds treated with an equal number of ASCs delivered in suspension [20]. Notwithstanding the successful application of MSC spheroids in tissue regeneration [16, 27], there are some drawbacks associated with this technique. First, if spheroids are too large, then core necrosis may develop, particularly after injection into ischemic tissue [27]. Second, transplantation of MSC spheroids by injection may result in additional tissue damage, because a large-bore needle is needed, and spheroids sustain greater shear forces during injection, leading to cell death. Third, inadvertent infusion of spheroids into larger vessels may result in vascular thrombosis and aggravate an existing ischemic condition. This report describes a technique of using spheroid-derived ASCs to enhance tissue regeneration, as an alternative to cell therapy using spheroids to circumvent its associated difficulties. Previous studies have reported improvements in wound healing by injecting monolayer MSCs into wounds [30–32]. On the contrary, we observed significant enhancement in wound healing rate only after treatment with spheroid-derived ASCs. These prior studies used 1.5–3 times as many MSCs as our injection studies used, and high levels of cell death were observed within a few days following cell transplantation into ischemic tissue [30, 32]. In this study, we showed that spheroid-derived ASCs can significantly enhance wound healing at lower therapeutic doses compared with dosages previously reported for monolayer ASCs.

We attribute the regenerative properties of spheroid-derived ASCs to increased ASC engraftment in the wound environment throughout the repair process. Enhanced cellular retention in the damaged tissue probably results from the increased chemotactic capacity of spheroid-derived ASCs secondary to *CXCR4* upregulation. Increased secretion of angiogenic growth factors in the ASCs also enhances neovascularization and wound healing in injured tissue. Moreover, ASCs also contribute to cutaneous regeneration by spontaneous site-specific differentiation into epithelial and endothelial lineages [15, 16]. Previous studies have reported the differentiation of transplanted ASCs into endothelial cells, keratinocytes, and pericytes within cutaneous wounds [30, 31]. The immunofluorescent staining used in this study revealed increased colocalization of ASCs in the presence of CD31 and pancytokeratin immunofluorescence cells in wounds treated with spheroid-derived ASCs, suggesting greater capacity for transdifferentiation into endothelial and epithelial lineages. Given our in vitro data, which demonstrate enhanced stemness gene expression in spheroid-derived ASCs, it is possible that these ASCs with enhanced plasticity contributed to the nonmesenchymal cell population within healing cutaneous wounds.

CONCLUSION

Our study demonstrates the therapeutic superiority of monolayer-expanded ASCs after a short period of spheroid formation, as compared with ASCs that are constantly cultured in monolayers. Spheroid-derived ASCs exhibited better expansion efficiency and lower senescence during in vitro culture, and they also showed higher expression of stemness markers, angiogenic growth factors, CXCR4, and MMPs. In a cutaneous wound model of nude mice, we observed faster wound healing, more ASC engraftment, higher capillary density, and ASC differentiation toward nonmesenchymal lineages after intralesional injection of spheroid-derived ASCs. Our results suggest that short-term spheroid formation of ASCs before monolayer expansion can nonchemically enhance their regenerative capacity by promoting stemness, angiogenesis, and chemotaxis, thus providing increased therapeutic potential for tissue regeneration.

AUTHOR CONTRIBUTIONS

N.-C.C.: conception and design, provision of study material, data analysis and interpretation, financial support, manuscript writing; S.-Y.C. and J.-R.L.: collection and assembly of data, data analysis and interpretation; T.-H.Y.: conception and design, financial support, administrative support, final approval of manuscript.

DISCLOSURE OF POTENTIAL CONFLICTS OF INTEREST

The authors indicate no potential conflict of interest.

REFERENCES

1 Gimble JM, Guilak F. Differentiation potential of adipose derived adult stem (ADAS) cells. Curr Top Dev Biol 2003;58:137–160.

2 Aust L, Devlin B, Foster SJ et al. Yield of human adipose-derived adult stem cells from liposuction aspirates. Cytotherapy 2004;6:7–14.

3 Fraser JK, Wulur I, Alfonso Z et al. Fat tissue: An underappreciated source of stem cells for biotechnology. Trends Biotechnol 2006;24:150–154.

4 Tsai CC, Su PF, Huang YF et al. Oct4 and Nanog directly regulate Dnmt1 to maintain self-renewal and undifferentiated state in mesenchymal stem cells. Mol Cell 2012;47:169–182.

5 Yew TL, Hung YT, Li HY et al. Enhancement of wound healing by human multipotent stromal cell conditioned medium: The paracrine factors and p38 MAPK activation. Cell Transplant 2011;20:693–706.

6 Baer PC, Griesche N, Luttmann W et al. Human adipose-derived mesenchymal stem cells in vitro: Evaluation of an optimal expansion medium preserving stemness. Cytotherapy 2010;12:96–106.

7 Park E, Patel AN. Changes in the expression pattern of mesenchymal and pluripotent markers in human adipose-derived stem cells. Cell Biol Int 2010;34:979–984.

8 Cho HH, Kyoung KM, Seo MJ et al. Overexpression of CXCR4 increases migration and proliferation of human adipose tissue stromal cells. Stem Cells Dev 2006;15:853–864.

9 Potapova IA, Brink PR, Cohen IS et al. Culturing of human mesenchymal stem cells as three-dimensional aggregates induces functional expression of CXCR4 that regulates adhesion to endothelial cells. J Biol Chem 2008;283:13100–13107.

10 Ringe J, Strassburg S, Neumann K et al. Towards in situ tissue repair: Human mesenchymal stem cells express chemokine receptors CXCR1, CXCR2 and CCR2, and migrate upon stimulation with CXCL8 but not CCL2. J Cell Biochem 2007;101:135–146.

11 Gimble JM, Bunnell BA, Guilak F. Human adipose-derived cells: An update on the transition to clinical translation. Regen Med 2012;7:225–235.

12 Go MJ, Takenaka C, Ohgushi H. Forced expression of Sox2 or Nanog in human bone marrow derived mesenchymal stem cells maintains their expansion and differentiation capabilities. Exp Cell Res 2008;314:1147–1154.

13 Vicente López MA, Vazquez Garcia MN, Entrena A et al. Low doses of bone morphogenetic protein 4 increase the survival of human adipose-derived stem cells maintaining their stemness and multipotency. Stem Cells Dev 2011;20:1011–1019.

14 Li Y, Yu X, Lin S et al. Insulin-like growth factor 1 enhances the migratory capacity of mesenchymal stem cells. Biochem Biophys Res Commun 2007;356:780–784.

15 Bartosh TJ, Ylostalo JH, Mohammadipoor A et al. Aggregation of human mesenchymal stromal cells (MSCs) into 3D spheroids enhances their antiinflammatory properties. Proc Natl Acad Sci USA 2010;107:13724–13729.

16 Bhang SH, Cho SW, La WG et al. Angiogenesis in ischemic tissue produced by spheroid grafting of human adipose-derived stromal cells. Biomaterials 2011;32:2734–2747.

17 Yeh HY, Liu BH, Hsu SH. The calcium-dependent regulation of spheroid formation and cardiomyogenic differentiation for MSCs on chitosan membranes. Biomaterials 2012;33:8943–8954.

18 Cheng NC, Wang S, Young TH. The influence of spheroid formation of human adipose-derived stem cells on chitosan films on stemness and differentiation capabilities. Biomaterials 2012;33:1748–1758.

19 Nambu M, Ishihara M, Nakamura S et al. Enhanced healing of mitomycin C-treated wounds in rats using inbred adipose tissue-derived stromal cells within an atelocollagen matrix. Wound Repair Regen 2007;15:505–510.

20 Amos PJ, Kapur SK, Stapor PC et al. Human adipose-derived stromal cells accelerate diabetic wound healing: Impact of cell formulation and delivery. Tissue Eng Part A 2010;16:1595–1606.

21 Cai L, Johnstone BH, Cook TG et al. Suppression of hepatocyte growth factor production impairs the ability of adipose-derived stem cells to promote ischemic tissue revascularization. Stem Cells 2007;25:3234–3243.

22 Ceradini DJ, Kulkarni AR, Callaghan MJ et al. Progenitor cell trafficking is regulated by hypoxic gradients through HIF-1 induction of SDF-1. Nat Med 2004;10:858–864.

23 Ratajczak MZ, Kucia M, Reca R et al. Stem cell plasticity revisited: CXCR4-positive cells expressing mRNA for early muscle, liver and neural cells 'hide out' in the bone marrow. Leukemia 2004;18:29–40.

24 Schioppa T, Uranchimeg B, Saccani A et al. Regulation of the chemokine receptor CXCR4 by hypoxia. J Exp Med 2003;198:1391–1402.

25 Bobis-Wozowicz S, Miekus K, Wybieralska E et al. Genetically modified adipose tissue-derived mesenchymal stem cells overexpressing CXCR4 display increased motility, invasiveness, and homing to bone marrow of NOD/SCID mice. Exp Hematol 2011;39:686–696 e684.

26 Huang W, Wang T, Zhang D et al. Mesenchymal stem cells overexpressing CXCR4 attenuate remodeling of postmyocardial infarction by releasing matrix metalloproteinase-9. Stem Cells Dev 2012;21:778–789.

27 Wang CC, Chen CH, Hwang SM et al. Spherically symmetric mesenchymal stromal cell bodies inherent with endogenous extracellular matrices for cellular cardiomyoplasty. Stem Cells 2009;27:724–732.

28 Pedroso DC, Tellechea A, Moura L et al. Improved survival, vascular differentiation and wound healing potential of stem cells co-cultured with endothelial cells. PLoS One 2011;6:e16114.

29 Hung SC, Pochampally RR, Hsu SC et al. Short-term exposure of multipotent stromal cells to low oxygen increases their expression of CX3CR1 and CXCR4 and their engraftment in vivo. PLoS One 2007;2:e416.

30 Rustad KC, Wong VW, Sorkin M et al. Enhancement of mesenchymal stem cell angiogenic capacity and stemness by a biomimetic hydrogel scaffold. Biomaterials 2012;33:80–90.

31 Sasaki M, Abe R, Fujita Y et al. Mesenchymal stem cells are recruited into wounded skin and contribute to wound repair by transdifferentiation into multiple skin cell type. J Immunol 2008;180:2581–2587.

32 Silva EA, Kim ES, Kong HJ et al. Material-based deployment enhances efficacy of endothelial progenitor cells. Proc Natl Acad Sci USA 2008;105:14347–14352.

See www.StemCellsTM.com for supporting information available online.